Chromone, a Privileged Scaffold for the Development of Monoamine Oxidase Inhibitors

ARTICLE *in* JOURNAL OF MEDICINAL CHEMISTRY · JUNE 2011

Impact Factor: 5.45 · DOI: 10.1021/jm2004267 · Source: PubMed

Journal of Medicinal Chemistry

ARTICLE

pubs.acs.org/jmc

Chromone, a Privileged Scaffold for the Development of Monoamine Oxidase Inhibitors†

Alexandra Gaspar,[‡,§] Tiago Silva,[‡] Matilde Yáñez,[∥] Dolores Vina,[∥] Franscisco Orallo,[∥] Francesco Ortuso,[⊥] Eugenio Uriarte,[§] Stefano Alcaro,[*,⊥] and Fernanda Borges[*,‡]

[‡]CIQUP/Departamento de Química e Bioquímica, Faculdade de Ciências, Universidade do Porto, 4169-007 Porto, Portugal

[§]Departamento de Química Orgánica and [∥]Departamento de Farmacología, Facultad de Farmacia, Universidad de Santiago de Compostela, 15782 Santiago de Compostela, Spain

[⊥]Dipartimento di Scienze Farmacobiologiche, Facoltà di Farmacia, Università "Magna Græcia" di Catanzaro, Campus Universitario "S. Venuta", Viale Europa, 88100 Catanzaro, Italy

ABSTRACT: Two series of novel chromone derivatives were synthesized and investigated for their ability to inhibit the activity of monoamine oxidase. The SAR data indicate that chromone derivatives with substituents in position 3 of γ-pyrone nucleus act preferably as MAO-B inhibitors, with IC_{50} values in the nanomolar to micromolar range. Almost all chromone 3-carboxamides display selectivity toward MAO-B. Identical substitutions on position 2 of γ-pyrone nucleus result in complete loss of activity in both isoforms (chromones **2**−**12** except **3** and **5**). Notably, chromone (**19**) exhibits an MAO-B IC_{50} of 63 nM, greater than 1000-fold selectivity over MAO-A, and behaves as a quasi-reversible inhibitor. Docking experiments onto the MAO binding of the most active compound highlight different interaction patterns among the isoforms A and B. The differential analysis of the solvation effects among the chromone isomers gave additional insight about the superior outline of the 3-substituted chromone derivatives.

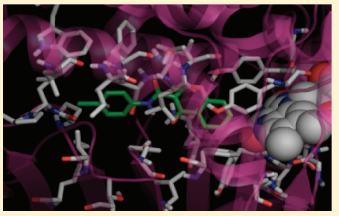

INTRODUCTION

Monoamine oxidases (MAOs, EC 1.4.3.4) are widely distributed enzymes that contain a flavin adenine dinucleotide (FAD) covalently bounded to a cysteine residue. Several living organisms possess MAOs that are responsible for the major neurotransmitter degrading in the central nervous system (CNS) and peripheral tissues.[1,2]

In mammals two isoforms of MAOs are present: MAO-A and MAO-B. Both isoforms are involved in the oxidative deamination of exogenous and endogenous amines, including neurotransmitters, thus modulating their concentrations in the brain and peripheral tissues.[1] The MAO-A enzyme is responsible for the deamination of the epinephrine, norepinephrine, and serotonin, whereas the MAO-B enzyme metabolizes β-phenethylamine.[1,3] The enzyme also plays an important role in the expression of toxicity of the Parkinsonism-producing neurotoxin 1-methyl-4-phenyl-1,2,3,6-tetrahydropyridine by bioactivation into the toxic metabolite, the 1-methyl-4-phenyl-1,2,3,6-tetrahydropyridinium ion.[3]

The MAO metabolic reaction involves the oxidation of the amine function via oxidative cleavage of the α-CH bond of the substrate with the ensuing generation of an imine intermediate. This pathway is accomplished by the reduction of the flavin cofactor that is reoxidized by molecular oxygen, with simultaneous hydrogen peroxide release. Subsequently, the imine intermediate is hydrolyzed by a nonenzymatic pathway yielding ammonia and the corresponding aldehyde (Scheme 1).[2]

Expression levels of MAO-B in neuronal tissue are enhanced 4-fold with aging, especially in glial cells, resulting in an increased level of dopamine metabolism and in the production of higher levels of hydrogen peroxide, which are thought to play a major role in the etiology of neurodegenerative diseases such as Parkinson's and Alzheimer's. MAO-B inhibitors are also currently in clinical trials for the treatment of Alzheimer's disease because an increased level of MAO-B has been detected in the plaque-associated astrocytes of brains from Alzheimer's patients.[4,5]

Today efforts toward the development of monoamine oxidase inhibitors are focused on selective MAO-A or MAO-B inhibitors. Selective MAO-B inhibitors, alone or combined with L-Dopa, are being examined in the treatment of, for example, schizophrenia, Alzheimer's disease, and Parkinson's disease. The MAO-A inhibitors are effective in the treatment of depression.

MAO-A is more sensitive to inhibition by clorgyline and moclobemide, and MAO-B is selectively inhibited by low concentrations of selegiline (*R*-(−)-deprenyl) and rasagiline (Scheme 2).[1,4]

All of these aspects have led to an intensive search for novel MAO inhibitors, and this effort has increased considerably in recent years. However, a large number of MAOs inhibitors introduced into clinical practice were discarded because of adverse effects, such as hepatotoxicity, orthostatic hypotension, and the so-called "cheese effect", which is characterized by hypertensive crises.[1] Currently, the MAO inhibitors of the new generation are usually characterized by their relative specificities for the MAO subtypes and in some cases by the reversibility of their actions.

Received: April 10, 2011
Published: June 22, 2011

dx.doi.org/10.1021/jm2004267 | *J. Med. Chem.* 2011, 54, 5165–5173

Scheme 1

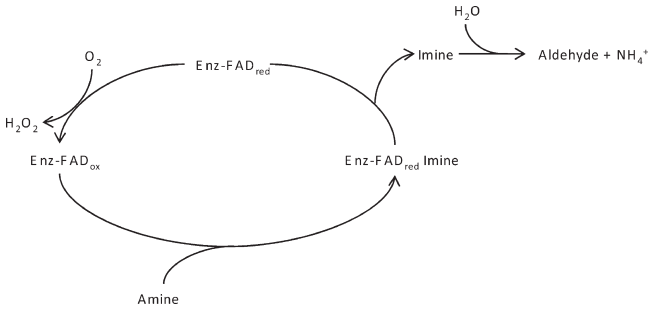

Scheme 2

Deprenyl Rasagiline

Despite considerable progress in understanding the interactions of the two enzyme forms with their preferred substrates and inhibitors, no general rules are yet available for the rational design of potent and selective inhibitors of MAO possibly because the mechanism of interaction of the new drugs with MAO isoforms has not been fully characterized.

Privileged structures such as indoles, arylpiperazines, biphenyls, and benzopyranes are currently ascribed as supportive approaches in drug discovery. Different families of nitrogen and oxygen heterocycles such as xanthones, coumarins, and their precursors (chalcones) have also been extensively used as scaffolds in medicinal chemistry programs for searching novel MAO-B inhibitors.[6−8]

Chromone scaffold [(4*H*)-1-benzopyran-4-one] has been recognized as a pharmacophore of a large number of bioactive molecules of either natural or synthetic origin. Until now, numerous biological effects, especially in popular medicine, have been ascribed to this benzo-γ-pyrone nucleus such as anti-inflammatory, antitumoral, and antimicrobial activities.[9] Enzymatic inhibition properties toward different systems such as oxidoreductases, kinases, tyrosinases, cyclooxygenases have also been recognized.[10] Recently, our group has reported preliminary studies that point out the relevance of these types of heterocyclic compound as monoamino oxidase inhibitors.[10,11]

Accordingly, our project has focused on the discovery of new chemical entities (NCEs) for MAO inhibition incorporating privileged structures with benzo-γ-pyrone substructure (Scheme 3). Preliminary studies performed with chromones (**1**) and (**13**) allow disclosure of the importance of the location of a carboxylic moiety in the γ-pyrone nucleus. In fact, when the −COOH substituent is in position 3 of the heterocyclic scaffold (**13**), it binds the *h*MAO-B, exerting a selective inhibition with respect to the A isoform (IC_{50}(*h*MAO-B) = 0.048 ± 0.0026 nM; MAO-B selective index (SI) of >2083).[10,11] As the inhibition is of irreversible type and in an attempt to develop novel reversible and selective MAO-B inhibitors, the synthesis of 2- and 3-carboxamide chromone derivatives capable of establishing hydrogen interactions with the enzyme was performed. Therefore, functionalized chromone scaffolds suitable to establish structure−activity relationships were obtained by synthetic strategies and screened toward human MAOs isoforms (*h*MAOs) to evaluate their potency/selectivity ratio. The Protein Data Bank (PDB)[12] availability of experimentally determined cocrystals of *h*MAO-A and -B with different kinds of ligand allows us to also perform structure-based molecular modeling studies with the aim to propose preferred binding modes and to explain the reasons of the isoform selectivity helping in the rational design of new inhibitors.

CHEMISTRY

The functionalization of the chromone nucleous leads to the obtention of two series of novel chromone carboxamides placed at positions C2 and C3 of the γ-pyrone ring. The compounds and the synthetic strategy used for their obtention have been patented[11] and are briefly depicted in Scheme 3. Chromone carboxamide derivatives were synthesized straightforwardly, in moderate/high yields, by a one-pot condensation reaction that occurs, in equimolar amounts, between the corresponding chromone carboxylic acid (**1** or **13**) and aniline (phenylamine) or its ring-substituted derivatives. A similar condensation reaction was performed with propylamine and cyclohexylamine. The coupling reagents selected for carboxylic acid activation were organophosphoric compounds, namely, (benzotriazol-1-yloxy)-tris(dimethylamino)phosphonium hexafluorophosphate (BOP) and (benzotriazol-1-yloxy)tripyrrolidinophosphonium hexafluorophosphate (PyBOP).[13] In all the reactions, *N*,*N*-diisopropylethylamine (DIPEA) was used instead of the classic triethylamine, since a significant increase of yield was observed due mainly to an improvement in the purification steps.[11]

It must be highlighted that the synthetic strategies commonly adopted for the synthesis of these types of amide are usually based on a different approach: first, an acyl halide is obtained through the reaction of a carboxylic acid with thionyl chloride, followed by the reaction with a nucleofilic agent.[14] In fact, the method herein presented is particularly advantageous, since it avoids the step of acyl halide obtention and the drawbacks related with this type of reagent. Furthermore, the use of BOP or PyBOP has several advantages, related with other coupling agents such as dicyclohexylcarbodiimide (DCC), in the purification steps and in the removal of side products. The syntheses of the dihydroxylated compounds **5** and **17** were performed by a demethylation reaction, using boron tribromide (BBr_3), of the monomethoxylated chromones **4** and **16**, respectively. The selected strategy avoids the prior protection of the hydroxyl groups of the starting materials (Scheme 3).

PHARMACOLOGY

The potential effects of the test drugs on *h*MAO activity were investigated by measuring their effects on the production of hydrogen peroxide (H_2O_2) from *p*-tyramine (a common substrate for both *h*MAO-A and *h*MAO-B), using the Amplex Red MAO assay kit (Molecular Probes, Inc., Eugene, OR, U.S.) and microsomal MAO isoforms prepared from insect cells (BTI-TN-5B1-4) infected with recombinant baculovirus containing cDNA inserts for *h*MAO-A or *h*MAO-B (Sigma-Aldrich Química S.A., Alcobendas, Spain).

The production of H_2O_2 catalyzed by MAO isoforms can be detected using 10-acetyl-3,7-dihydroxyphenoxazine (Amplex Red reagent), a nonfluorescent and highly sensitive probe that reacts with H_2O_2 in the presence of horseradish peroxidase to produce a fluorescent product, resorufin.

dx.doi.org/10.1021/jm2004267 |*J. Med. Chem.* 2011, 54, 5165–5173

Scheme 3[a]

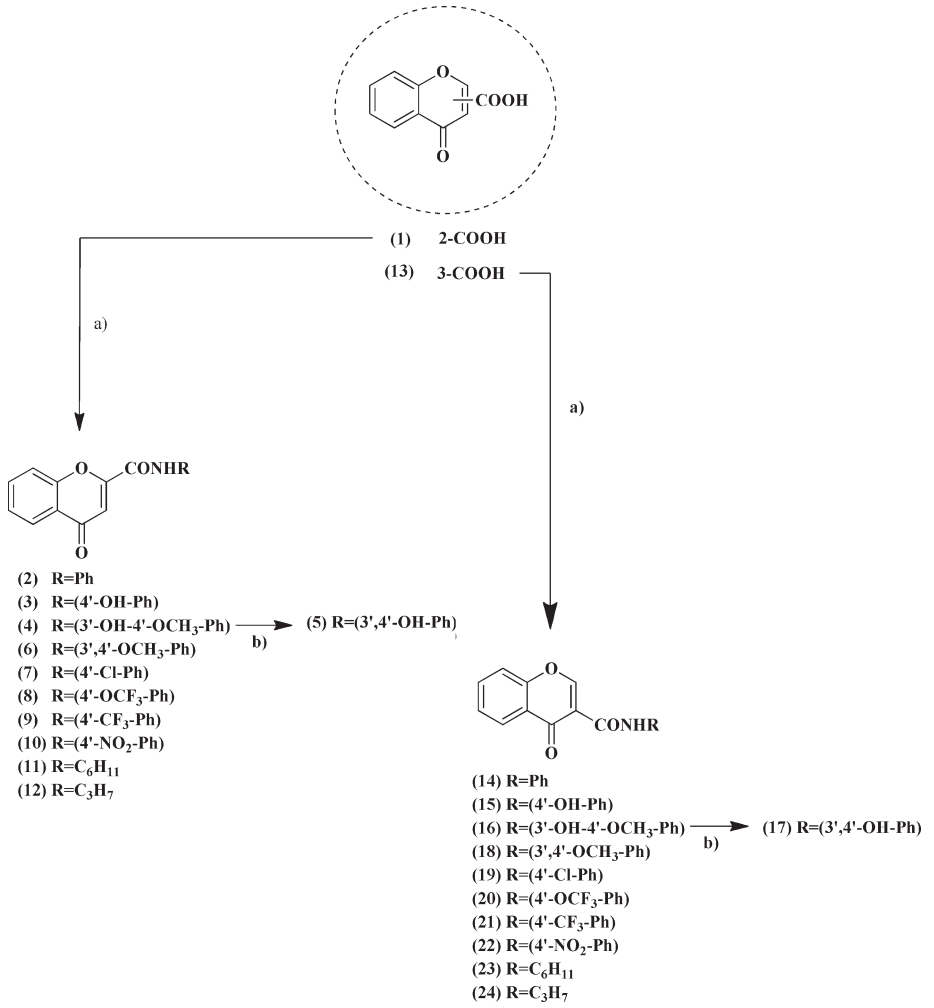

[a] Reagents: (a) RNH_2, BOP or PyBOP, DIPEA in DCM/DMF; (b) BBr_3 in DCM.

In this study, *h*MAO activity was evaluated using the above-mentioned method following the general procedure previously described elsewhere.[8,15] The drugs (novel compounds and reference inhibitors) were unable to react directly with the Amplex Red reagent, which indicates that they do not interfere with the measurements.

In our experiments and under our experimental conditions, *h*MAO-A displayed a Michaelis constant (K_m) of 457.17 ± 38.62 μM and a maximum reaction velocity (V_{max}) of 185.67 ± 12.06 (nmol/min)/mg protein whereas *h*MAO-B showed a K_m of 220.33 ± 32.80 μM and a V_{max} of 24.32 ± 1.97 (nmol/min)/mg protein (n = 5).

The *h*MAO-A and *h*MAO-B inhibition and SI ([IC_{50} (MAO-A)]/[IC_{50} (MAO-B)]) data are reported in Table 1.

Reversibility and irreversibility experiments were performed to evaluate the type of the inhibitor, using *R*-(−)deprenyl (irreversible inhibitor) and isatin (reversible inhibitor) as standards.[16]

RESULTS AND DISCUSSION

The chemical structures of the examined compounds are depicted in Scheme 3. The results of the in vitro evaluation of inhibitory potencies toward *h*MAO isoforms and selectivity of the chromones under study, and reference compounds, are shown in Table 1. By analyzing such data, one can conclude that chromones bearing substituents in position 3 of γ-pyrone nucleus act preferably as MAO-B inhibitors (iMAO-B) with IC_{50} values in the nanomolar to micromolar range. The same tendency was found with the chromone carboxylic acids.[10] The most promising iMAO-B chromones that are substituted in the para position, with hydroxyl or methoxyl groups or a chloro atom, of the side chain aromatic nucleus (compounds **15, 16** and **19**, respectively) present IC_{50} values between 63 and 76 nM. The most selective compounds possess electron withdrawing groups (a Cl atom (compound **19**) and a CF_3 group (compound **21**)) in the para position of the exocyclic aromatic nucleus (SI of >1.585 and >909, respectively). The chromone derivative with a hydroxyl group in the para position (compound **15**) is more active and selective as iMAO-B than the compound with two hydroxyl groups located in the para and meta positions (compound **17**). The present results allow us to point out that the inclusion of this type of substituent in the meta position of the 3-aryl substituent could not be beneficial. The derivative **22** with the para position substituted with a strong electron polar and bulky withdrawing group (nitro group) shows a loss of selectivity with an IC_{50}

dx.doi.org/10.1021/jm2004267 |*J. Med. Chem.* 2011, 54, 5165–5173

Table 1. MAO Inhibitory Activities of Chromone Carboxamides and Reference Inhibitors[a]

compd	R	IC_{50}(hMAO-A) (μM)	IC_{50}(hMAO-B) (μM)	SI
2	Ph	c	c	
3	4′-OH-Ph	65.23 ± 5.82	41.90 ± 2.79	1.6
4	3′-OH-4′-OCH_3-Ph	c	c	
5	3′,4′-OH-Ph	0.19 ± 0.016	2.66 ± 0.13	0.071
6	3′,4′-OCH_3-Ph	c	c	
7	4′-Cl-Ph	c	c	
8	4′-OCF_3-Ph	c	c	
9	4′-CF_3-Ph	c	c	
10	4′-NO_2-Ph	c	c	
11	C_6H_{11}	c	d	
12	C_3H_7	c	d	
14	Ph	c	0.40 ± 0.022	>250[e]
15	4′-OH-Ph	4.76 ± 0.39[b]	0.064 ± 0.0054	74
16	3′-OH-4′-OCH_3-Ph	8.34 ± 0.27[b]	0.076 ± 0.0032	110
17	3′,4′-OH-Ph	0.43 ± 0.0035b	0.16 ± 0.013	2.7
18	3′,4′-OCH_3-Ph	c	2.33 ± 0.07	>43[e]
19	4′-Cl-Ph	c	0.063 ± 0.0042	>1585[e]
20	4′-OCF_3-Ph	c	1.08 ± 0.072	>93[e]
21	4′-CF_3-Ph	c	0.11 ± 0.0074	>909 [e]
22	4′-NO_2-Ph	11.11 ± 0.74	11.78 ± 0.79	0.94
23	C_6H_{11}	c	0.93 ± 0.062	>107[e]
24	C_3H_7	c	37.69 ± 1.68	>2.7[e]
R-(−)-deprenyl		68.73 ± 4.21[b]	0.017 ± 0.0019	4043
iproniazid		6.56 ± 0.76	7.54 ± 0.36	0.87

[a] All IC_{50} values shown in this table are the mean ± SEM from five experiments. SI: *h*MAO-B selectivity index = IC_{50}(*h*MAO-A)/IC_{50}(*h*MAO-B). [b] Level of statistical significance: $P < 0.01$ versus the corresponding IC_{50} values obtained against MAO-B, as determined by Student's *t* test. The IC_{50} values of compounds **2** and **14** were taken from the literature.[11c] [c] Inactive at 100 μM (highest concentration tested). [d] Inactive at 1 mM (highest concentration tested). [e] Values obtained under the assumption that the corresponding IC_{50} against MAO-A or MAO-B is the highest concentration tested (100 μM or 1 mM).

of 11 μM for both MAO isoforms. It seems that the electron withdrawing nature, in particular the resonance effect (weak donating), and the spatial volume of the substituents located in the aromatic ring have a particular effect on the potency of the 3-carboxamides.

The chromone carboxamide derivative with an unsubstituted exocyclic aromatic moiety (compound **14**) is twice more active than compound **23**, a carboxamide with a cyclohexyl instead of the aromatic ring (IC_{50} of 400 and 930 nM, respectively). The absence of a ring led to a dramatic loss of activity (see linear alkylcarboxamide **24**; IC_{50} of 37 μM). All of the previously mentioned chromone carboxamides, except chromone **22**, are inactive toward MAO-A.

Of note is that the chromones bearing the same type of substituents in position 2 of γ-pyrone nucleus (chromones **2**−**12**) present a total loss of MAO inhibition except with compounds **3** and **5**. Compound **3**, with a hydroxyl group in the para position of the exocyclic aromatic ring, has a comparable inhibitory activity for both isoforms. The introduction of another hydroxyl group in the meta position (compound **5**) considerably increases the potency and selectivity toward *h*MAO-A.

The reversibility studies performed with the chromones **15** and **19** revealed that the carboxamides behave as quasi-reversible MAO-B inhibitors. In fact, the percent of enzymatic inhibition was much lower after repeated washing with respect to *R*-(−)-deprenyl (irreversible inhibitor) (Table 2).

Table 2. Reversibility and Irreversibility of *h*MAO Inhibition[a]

	% *h*MAO-B inhibition	
compd	before washing	after repeated washing
R-(−)-deprenyl (25 nM)	53.62 ± 5.15	47.72 ± 6.21
isatin (20 μM)	47.55 ± 5.42	0[b]
15 (100 nM)	60.31 ± 7.74	23.50 ± 3.71[b]
19 (100 nM)	59.60 ± 6.96	29.14 ± 4.16

[a] Each value is the mean ± SEM from five experiments ($n = 5$). [b] Level of statistical significance: $P < 0.05$ versus the corresponding % hMAO-B inhibition before washing, as determined by Student's *t* test.

The data so far obtained are in accordance with preliminary results,[11] since it supports the assumption that the positive hydrophobicity ($+\pi$) of the substituent, besides inductive and mesomeric effects, located on the phenyl exocyclic moiety markedly influences the potency and selectivity of the chromone carboxamides. The tendency is in perfect agreement with the parameter space of the descriptors defined in the so-called Craig's plot.

In order to highlight the reasons of MAO selectivity, we have carried out a structure-based molecular modeling study using *h*MAOs cocrystals deposited into the PDB.[12] Similar to our previous work,[17] we have focused our attention onto the most active and

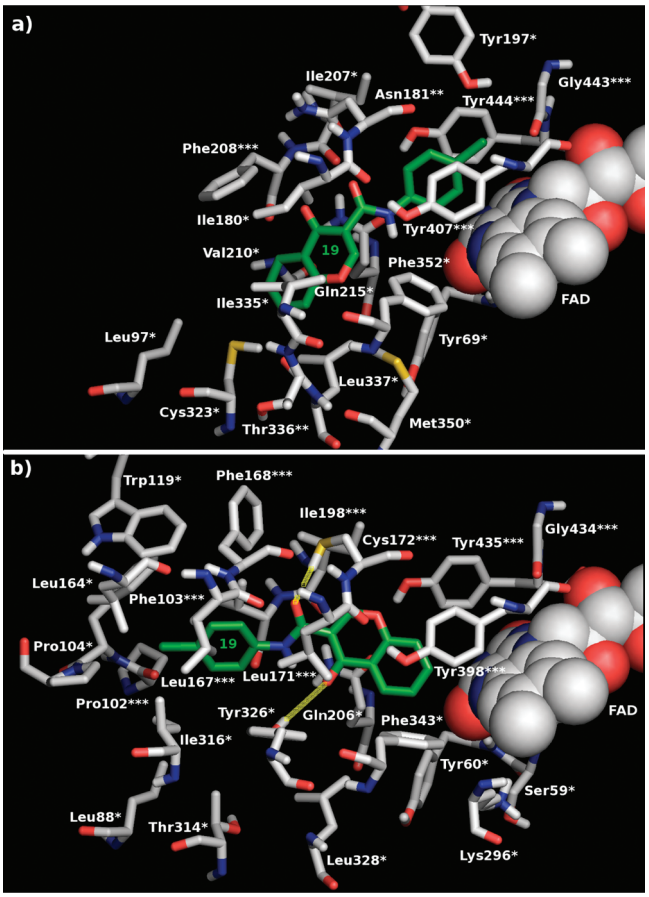

Figure 1. Most stable docking poses of **19** into (a) *h*MAO-A and (b) *h*MAO-B binding sites. Ligand is reported in green carbon sticks. Interacting residues are in gray carbon sticks, and FAD is in space-fill. Yellow dotted lines indicate ligand−enzyme intermolecular hydrogen bonds: ∗, ligand interaction to side chain; ∗∗, ligand interaction to backbone; ∗∗∗, ligand interaction to both backbone and side chain.

selective compound. So in this series, we have selected **19** as a case study for our theoretical investigation. Also in the present study we have adopted the docking program Glide[18] and the PDB models 2Z5X[19] and 2V5Z[20] for mimicking the *h*MAO-A and -B targets, respectively. Details of the molecular modeling procedures are reported in the Experimental Section.

Compound **19** target interaction energies, −7.12 and −207.68 kJ/mol for *h*MAO-A and -B, respectively, were in good agreement with the experimental biological data. The docking proposed configuration indicated a strong difference depending on the target. Actually, the only [*h*MAO-A·**19**] Glide proposed configuration showed the chromone moieties in the entrance gorge while the *p*-cloroanilide side chain recognized the FAD cofactor suggesting a $\pi-\pi$ interaction to Tyr407 and Tyr444. Several other residues were involved in such a binding mode but only van der Waals contacts can be designated (Figure 1a).

The interaction of **19** to *h*MAO-B was found to be much more productive with respect to the previous one. First of all, the interaction energy was remarkably lower than in *h*MAO-A and a number of binding modes were proposed by Glide. Moreover, the most stable configuration was in agreement with literature data as concerns the intramolecular hydrogen bond and with the positioning of the chromone ring.[17] Actually, the chromone

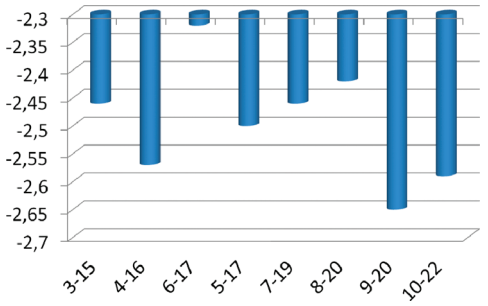

Figure 2. Difference (in kJ/mol) between water solvation energies of **3**−**10** with respect to their isomers **15**−**22**.

moiety was situated close to the FAD and the *p*-cloroanilide side chain occupied the entrance cavity at the loop formed by residues 99−112. Two intermolecular hydrogen bonds were observed between the carboxyamide and the Cys172 and between the chromone sp^2 oxygen and the Tyr326. The hydrophobic side chain of **19** productively interacts with Pro102, Phe103, Leu167, and Ile199.

With the aim to more deeply investigate the reasons for the different recognition of **19** in *h*MAO-A with respect to the *h*MAO-B, the best docking poses, reported in Figure 1b, were superposed using the FAD and the active site backbone residues as geometry references. Such a procedure indicated that *h*MAO-B configuration of **19** in *h*MAO-A loses the hydrogen bond contribution because Cys172 and Tyr326, available into the former enzyme, are replaced by Asn181 and Ile335, respectively. Moreover, in the *h*MAO-A cleft the **19** *p*-cloroanilide moiety bumps against the side chain of Phe208 corresponding to the sterically smaller *h*MAO-B Ile199. The same analysis has been carried out on the **19** *h*MAO-A best pose with respect to *h*MAO-B. In this case we can report clashes between the chromone moiety and the Tyr326 and no hydrogen bond. In order to reduce clashes, both new models have been refined with Glide software, but after the optimization the scenario was not so different: the clashes were reduced, but with respect to the docking best poses, the inhibitor was located more distant from the FAD and no intermolecular hydrogen bonds were established between the ligand and the targets.

After the docking experiments with the most active and selective compound we have repeated the same procedure trying to reproduce by interaction energies the biological trend reported in Table 1, at least for the quantitatively measured values. Since no good correlation was found for the entire set, we have focused our attention onto the conformational and solvation properties of our derivatives. In particular a comparison of the isomers bearing the side chain at the 2- or 3-position onto the chromone ring has been carried out. The conformational properties, investigated by means of Monte Carlo (MC) search, indicated few possible local minimum energy structures in particular for compounds **15**−**22**. Such data could be considered as an entropy benefit of these ligands with respect to their isomers **3**−**10**. The comparative solvation analysis in water revealed a remarkable energy advantage of compounds **3**−**10** with respect to their isomers **15**−**22** (Figure 2). Such evidence could contribute to explain the better activity of chromone derivatives reporting the carboxyamide side chain at position 3 than at position 2. In fact, the interaction with the target of **3**−**10** could be penalized into the aqueous environment.

dx.doi.org/10.1021/jm2004267 |*J. Med. Chem.* 2011, 54, 5165–5173

CONCLUSIONS

In the present work evidence was acquired to demonstrate that chromone is a valid scaffold for the design of potent, selective, and reversible MAO inhibitors. Generally chromones bearing substituents in position 3 of γ-pyrone nucleus act as *h*MAO-B selective inhibitors and those bearing substituents in position 2 of the same nucleus selectively inhibit the *h*MAO-A or are inactive. The introduction of a chloro substituent in the para position of the exocyclic aromatic ring of chromone 3-phenylcarboxamides was crucial for the obtention of a potent and selective iMAO (IC_{50} = 63 nM; SI > 1585). The easy synthetic accessibility and potentially low toxicity of chromones[9] make them "privileged" scaffolds. Docking experiments, carried out with the most active and selective compound **19**, indicated the reasons for the better stabilization within the *h*MAO-B isoform versus the -A one. A comparison of **3**−**10** and **15**−**22** conformational properties indicated an entropy advantage of the latter in the interaction with both targets. The solvation energies comparison reported a preference of the 2-substituted chromone derivatives for the aqueous solvent. Both results suggested a penalization of **3**−**10** in target recognition with respect to **15**−**22**.

Additional studies are warranted for a systematic lead optimization, modulated by appropriate modifications of length, size, and chemical nature of the substituents, a process that can lead to in the future to a drug candidate.

EXPERIMENTAL SECTION

Chemistry. Chromone-2-carboxylic and chromone-3-carboxylic acids, benzotriazol-1-yloxy)tris(dimethylamino)phosphonium hexafluorophosphate (BOP), benzotriazol-1-yloxy)tripyrrolidinophosphonium hexafluorophosphate (PyBOP), *N*,*N*-diisopropylethylamine (DIPEA), dimethylformamide (DMF), boron tribromide (BBr_3), and aniline and its derivatives were purchased from Sigma-Aldrich Química S.A. (Sintra, Portugal). All other reagents and solvents were pro analysis grade and were acquired from Merck (Lisbon, Portugal) and used without additional purification.

Thin-layer chromatography (TLC) was carried out on precoated silica gel 60 F254 (Merck) with layer thickness of 0.2 mm. For analytical control the following systems were used: ethyl acetate/petroleum ether, ethyl acetate/methanol, and chloroform/methanol in several proportions. The spots were visualized under UV detection (254 and 366 nm) and iodine vapor. Normal-phase column chromatography was performed using silica gel 60, 0.2−0.5 or 0.040−0.063 mm (Merck).

Following the workup and after extraction, the organic phases were dried over Na_2SO_4. Solutions were decolorized with activated charcoal when necessary. The recrystallization solvents were ethyl acetate or ethyl ether/*n*-hexane. Solvents were evaporated in a Buchi Rotavapor.

The purity of the final products (>97% purity) was verified by high-performance liquid chromatography (HPLC) equipped with a UV detector. Chromatograms were obtained in an HPLC/DAD system, a Jasco instrument (pump model 880-PU and solvent mixing model 880-30, Tokyo, Japan) equipped with a commercially prepacked Nucleosil RP-18 analytical column (250 mm × 4.6 mm, 5 μm, Macherey-Nagel, Duren, Germany) and UV detection (Jasco model 875-UV) at the maximum wavelength of 254 nm. The mobile phase consisted of a methanol/water or acetonitrile/water (gradient mode, room temperature) at a flow rate of 1 mL/min. The chromatographic data were processed in a Compaq computer fitted with CSW 1.7 software (DataApex, Czech Republic).

Apparatus. ^{1}H NMR data were acquired, at room temperature, on a Brüker AMX 300 spectrometer operating at 300.13 MHz. Dimethylsulfoxide-d_6 was used as a solvent. Chemical shifts are expressed in δ (ppm) values relative to tetramethylsilane (TMS) as internal reference. Coupling constants (J) are given in Hz. Electron impact mass spectrometry (EI-MS) was carried out on a VG AutoSpec instrument. The data are reported as m/z (% of relative intensity of the most important fragments). Melting points were obtained on a Stuart Scientific SMP1 apparatus and are uncorrected.

Synthesis. General Procedure for Amide Obtention. The synthetic procedure corresponds to a one-pot condensation reaction that occurs, in equimolar amounts, between the carboxylic acid and the respective amine according to the following general procedure. 2-Carboxychromone (**1**) or 3-carboxychromone (**13**) (0.50 g, 2.63 mmol) was dissolved in 6 mL of DMF and 0.37 mL of diisopropylethylamine (DIPEA). The solution was then cooled at 0 °C in an ice−water bath, and a BOP (1.16 g, 2.63 mmol) or PyBOP (1.37 g, 2.63 mmol) solution in CH_2Cl_2 (6 mL) was added. The mixture was stirred for 30 min. Afterward, the corresponding amine (phenylamine, 4-hydroxyphenylamine, 3-hydroxy-4-methoxyphenylamine, 3,4-dimethoxyphenylamine, cyclohexylamine, or propylamine) was added in equimolar amount. The temperature was gradually increased to room temperature. The mixture was stirred for additional 4 h.

General Procedure for Demethylation Reactions. The monomethoxylated chromone carboxamide **4** or **16** (0.25 g, 0.80 mmol) was suspended in anhydrous dichloromethane and under argon atmosphere. The resulting suspension was stirred, cooled at −80 °C, and BBr_3 (6 mL of a 1 M solution in dicloromethane) was added dropwise. Once the addition was completed, the reaction mixture was allowed to warm to room temperature with continuous stirring. After BBr_3 destruction with methanol, the purification process was carried out straightforwardly.

The structural elucidation of the other carboxamides was described elsewhere.

***N*-(3,4-Dihydroxyphenyl)-4-oxo-4*H*-1-benzopyran-2-carboxamide (5).** Yield: 65%. Mp: 267−271 °C. ^{1}H NMR: δ = 6.75 (1H, d, J = 8.5, H(5′)), 6.94 (1H, s, H(3)), 7.04 (1H, dd, J = 8.5, 2.4, H(6′)), 7.32 (1H, d, J = 2.4, H(2′)), 7.58 (1H, ddd, J = 8.0, 6.8, 1.2, H(6)), 7.85 (1H, d, J = 8.0, H(8)), 7.93 (1H, ddd, J = 8.5, 7.0, 1.5, H(7)), 8.08 (1H, dd, J = 7.6, 1.4, H(5)), 8.94 (1H, s, 3′-OH), 9.17 (1H, s, 4′-OH), 10.49 (1H, s, CONH). EI-MS m/z: 298 (10), 297 ($M^{+\bullet}$, 52), 296 (19), 146 (100), 124 (92), 105 (57), 97 (16), 89 (74), 77 (15), 69 (19), 68 (15), 63 (16).

***N*-(4-(Chlorophenyl)-4-oxo-4*H*-1-benzopyran-2-carboxamide (7).** Yield: 50%. Mp: 268−271 °C. ^{1}H NMR: δ = 6.97 (1H, s, H(3)), 7.48 (2H, d, J = 8.8, H(3′), H(5′)), 7.56 (1H, m, H(6)), 7.83−7.96 (4H, m, H(7), H(8), H(2′), H(6′)), 8.08 (1H, dd, J = 7.9, 1.6, H(5)), 10.87 (1H, s, CONH). EI-MS m/z: 301 (34), 300 (33), 299 ($M^{+\bullet}$, 100), 298 (50), 282 (15), 270 (24), 173 (14), 145 (28), 101 (18), 90 (10), 89 (89), 69 (16), 63 (14).

***N*-(4-(Trifluoromethoxy)phenyl)-4-oxo-4*H*-1-benzopyran-2-carboxamide (8).** Yield: 56%. Mp: 241−244 °C. ^{1}H NMR: δ = 7.00 (1H, s, H(3)), 7.45 (2H, d, J = 8.2, H(3′), H(5′)), 7.57 (1H, dd, J = 8.2, 7.4, H(6)), 7.90−7.97 (4H, m, H(7), H(8), H(2′), H(6′)), 8.08 (1H, d, J = 7.6, H(5)), 10.92 (1H, s, CONH). EI-MS m/z: 349 ($M^{+\bullet}$, 86), 348 (100), 332 (21), 320 (41), 264 (12), 176 (17), 173 (21), 145 (44), 117 (18), 101 (20), 89 (98), 69 (24).

***N*-(4-(Trifluoromethyl)phenyl)-4-oxo-4*H*-1-benzopyran-2-carboxamide (9).** Yield: 50%. Mp: 258−261 °C. ^{1}H NMR: δ = 7.02 (1H, s, H(3)), 7.58 (1H, ddd, J = 8.1, 7.0, 1.2, H(6)), 7.81 (2H, d, J = 8.8, H(3′), H(5′)), 7.86 (1H, dd, J = 8.4, 1.0, H(8)), 7.94 (1H, ddd, J = 8.6, 7.0, 1.6, H(7)), 8.06 (2H, d, J = 8.4, H(2′), H(6′)), 8.09 (1H, dd, J = 7.6, 1.6, H(5)), 11.04 (1H, s, CONH). EI-MS m/z: 333 ($M^{+\bullet}$, 35), 332 (100), 303 (16), 173 (15), 145 (32), 117 (12), 101 (11), 89 (58), 69 (15), 57 (12).

***N*-(4-Nitrophenyl)-4-oxo-4*H*-1-benzopyran-2-carboxamide (10).** Yield: 15%. Mp: >280 °C. ^{1}H NMR: δ = 7.04 (1H, s, H(3)), 7.59 (1H, ddd, J = 8.2, 7.0, 1.2, H(6)), 7.86 (1H, d, J = 7.6, H(8)), 7.96 (1H, ddd, J = 8.6, 7.0, 1.6, H(7)), 8.10 (3H, m, H(5), H(2′), H(6′)), 8.34 (2H, m, H(3′), H(5′)), 11.22 (1H, s, CONH). EI-MS m/z: 310 ($M^{+\bullet}$, 6), 309

(22), 123 (45), 111 (38), 101 (45), 99 (54), 97 (69), 95 (32), 87 (63), 85 (90), 83 (51), 73 (74), 71 (69), 69 (56), 58 (35), 57 (100), 55 (65).

***N*-Cyclohexyl-4-oxo-4*H*-1-benzopyran-2-carboxamide (11).** Yield: 60%. Mp: 183−184 °C. ^{1}H NMR: δ = 1.12−1.86 (10H, m, 2 × H(2′), 2 × H(3′), 2 × H(4′), 2 × H(5′), 2 × H(6′)), 3.78 (1H, m, H(1′)), 6.83 (1H, s, H(3)), 7.54 (1H, dd, *J* = 7.9, 7.2, H(6)), 7.79 (1H, d, *J* = 8.4, H(8)), 7.90 (1H, ddd, *J* = 8.5, 7.0, 1.4, H(7)), 8.05 (1H, d, *J* = 7.9, H(5)), 8.88 (1H, d, *J* = 8.1, CONH). EI-MS *m*/*z*: 271 ($M^{+\bullet}$, 38), 228 (12), 191 (19), 190 (100), 173 (16), 145 (12), 89 (39).

***N*-Propyl-4-oxo-4*H*-1-benzopyran-2-carboxamide (12).** Yield: 84%. Mp: 167−171 °C. ^{1}H NMR ($CDCl_3$): δ = 1.02 (3H, *t*, *J* = 7.4, CH_3), 1.70 (2H, m, CH_3CH_2), 3.47 (2H, m, $NHCH_2$), 7.02 (1H, bs, CONH), 7.17 (1H, s, H(3)), 7.46 (1H, ddd, *J* = 8.0, 7.0, 1.0, H(6)), 7.53 (1H, dd, *J* = 7.9, 1.0, H(8)), 7.74 (1H, ddd, *J* = 8.6, 7.0, 1.3, H(7)), 8.22 (1H, dd, *J* = 8.0, 1.6, H(5)). EI-MS *m*/*z*: 232 (16), 231 ($M^{+\bullet}$, 100), 216 (26), 203 (12), 202 (22), 190 (10), 189 (30), 174 (19), 173 (93), 159 (20), 146 (12), 145 (43), 101 (15), 89 (83), 69 (17), 63 (11).

***N*-(3,4-Dihydroxyphenyl)-4-oxo-4*H*-1-benzopyran-3-carboxamide (17).** Yield: 50%. Mp: 266−269 °C. ^{1}H NMR: δ = 6.82 (1H, d, *J* = 8.4, H(5′)), 6.94 (1H, dd, *J* = 8.5, 2.4, H(6′)), 6.99 (1H, d, *J* = 2.5, H(2′)), 7.33−7.39 (2H, m, H(6), H(8)), 7.69 (1H, dd, *J* = 8.4, 7.1, H(7)), 7.99 (1H, dd, *J* = 7.7, 1.3, H(5)), 8.64 (0.7H, s, H(2)), 8.68 (0.7H, s, H(2)), 8.72 (0.3H, s, H(2)), 9.43 (1H, s, OH), 9.46 (1H, s, OH), 11.73 (0.3H, s, CONH), 11.80 (0.3H, s, CONH), 13.42 (0.7H, s, CONH), 13.46 (0.7H, s, CONH). EI-MS *m*/*z*: 297 ($M^{+\bullet}$, 7), 281 (11), 208 (13), 207 (73), 173 (100), 149 (24), 121 (72), 97 (20), 95 (27), 83 (27), 81 (33), 77 (21), 73 (36), 71 (26), 69 (40), 55 (57).

***N*-(4-(Chlorophenyl)-4-oxo-4*H*-1-benzopyran-3-carboxamide (19).** Yield: 47%. Mp: 255−259 °C. ^{1}H NMR: δ = 7.34 (1H, d, *J* = 7.8, H(8)), 7.38 (1H, dd, *J* = 7.6, 1.3, H(6)), 7.54 (2H, d, *J* = 8.8, H(3′), H(5′)), 7.70−7.73 (3H, m, H(2′), H(6′), H(7)), 7.99 (1H, dd, *J* = 7.8, 1.5, H(5)), 8.85 (0.7H, d, *J* = 13.8, H(2)), 8.88 (0.3H, d, *J* = 14.8, H(2)), 8.88 (0.3H, d, *J* = 14.8, H(2)), 11.84 (0.3H, d, *J* = 14.8, CONH), 11.84 (0.3H, d, *J* = 14.8, CONH), 13.39 (0.7H, d, *J* = 13.8, CONH). EI-MS *m*/*z*: 301 (37), 300 (21), 299 ($M^{+\bullet}$, 88), 174 (16), 173 (100), 151 (18), 121 (37), 92 (11), 89 (10).

***N*-(4-(Trifluoromethoxy)phenyl)-4-oxo-4*H*-1-benzopyran-3-carboxamide (20).** Yield: 55%. Mp: 223−226 °C. ^{1}H NMR: δ = 7.31−7.38 (2H, m, H(6), H(8)), 7.46 (2H, d, *J* = 8.7, H(3′), H(5′)), 7.71 (1H, ddd, *J* = 8.5, 7.0, 1.5, H(7)), 7.79 (2H, d, *J* = 8.7, H(2′), H(6′)), 8.00 (1H, dd, *J* = 7.8, 1.5, H(5)), 8.85 (0.7H, d, *J* = 13.5, H(2)), 8.89 (0.3H, d, *J* = 15.3, H(2)), 11.84 (0.3H, d, *J* = 15.2, CONH), 13.42 (0.7H, d, *J* = 13.5, CONH). EI-MS *m*/*z*: 349 ($M^{+\bullet}$, 31), 201 (13), 174 (12), 173 (100), 121 (30), 92 (10).

***N*-(4-(Trifluoromethyl)phenyl)-4-oxo-4*H*-1-benzopyran-3-carboxamide (21).** Yield: 55%. Mp: 251−254 °C. ^{1}H NMR: δ = 7.36 (1H, d, *J* = 8.0, H(8)), 7.39 (1H, dd, *J* = 8.0, 1.7, H(6)), 7.73 (1H, ddd, *J* = 8.3, 7.6, 1.6, H(7)), 7.83−7.92 (4H, m, H(2′), H(3′), H(5′), H(6′)), 8.00 (1H, dd, *J* = 7.8, 1.4, H(5)), 8.95 (0.7H, d, *J* = 13.7, H(2)), 8.98 (0.3H, d, *J* = 14.6, H(2)), 11.90 (0.3H, d, *J* = 14.6, CONH), 13.40 (0.7H, d, *J* = 13.7, CONH). EI-MS *m*/*z*: 333 ($M^{+\bullet}$, 58), 212 (11), 185 (19), 173 (100), 145 (15), 121 (33), 92 (13).

***N*-(4-Nitrophenyl)-4-oxo-4*H*-1-benzopyran-3-carboxamide (22).** Yield: 35%. Mp: >280 °C. ^{1}H NMR: δ = 7.35−7.41 (2H, m, H(6), H(8)), 7.74 (1H, ddd, *J* = 8.2, 7.3, 1.7, H(7)), 7.93−7.96 (2H, m, H(2′), H(6′)), 8.00 (1H, dd, *J* = 7.9, 1.6, H(5)), 8.32 (2H, d, *J* = 9.2, H(3′), H(5′)), 8.97 (0.7H, d, *J* = 13.5, H(2)), 8.99 (0.3H, d, *J* = 14.3, H(2)), 11.94 (0.3H, d, *J* = 14.2, CONH), 13.39 (0.7H, d, *J* = 13.3, CONH). EI-MS *m*/*z*: 310 ($M^{+\bullet}$, 34), 309 (18), 280 (15), 173 (100), 123 (20), 121 (45), 116 (16), 109 (16).

***N*-Cyclohexyl-4-oxo-4*H*-1-benzopyran-3-carboxamide (23).** Yield: 30%. Mp: 181−184 °C. ^{1}H NMR: δ = 1.32−1.94 (10H, m, 2 × H(2′), 2 × H(3′), 2 × H(4′), 2 × H(5′), 2 × H(6′)), 3.70 (1H, m, H(1′)), 7.32 (2H, m, H(6), H(8)), 7.66 (1H, dd, *J* = 8.0, 7.3, H(7)), 8.02 (0.7H, d, *J* = 7.6, H(5)), 8.11 (0.3H, d, *J* = 7.6, H(5)), 8.44 (0.7H, d, *J* = 14.8, H(2)), 8.60 (0.3H, d, *J* = 14.8, H(2)), 10.31 (0.3H, brs, CONH), 11.85 (0.7H, brs, CONH). EI-MS *m*/*z*: 271 ($M^{+\bullet}$, 100), 228 (18), 188 (23), 175 (23), 173 (18), 121 (31), 97 (22), 57 (17).

***N*-Propyl-4-oxo-4*H*-1-benzopyran-3-carboxamide (24).** Yield: 18%. Mp: 139−142 °C. ^{1}H NMR: δ = 1.04 (3H, m, CH_3), 1.77 (2H, m, CH_3CH_2), 3.52 (2H, m, $NHCH_2$), 7.23−7.30 (2H, m, H(6), H(8)), 7.57 (1H, ddd, *J* = 8.5, 7.0, 1.5, H(7)), 8.03 (0.7H, d, *J* = 7.6, H(5)), 8.10 (0.3H, d, *J* = 7.7, H(5)), 8.40 (0.7H, d, *J* = 15.0, H(2)), 8.55 (0.3H, d, *J* = 15.0, H(2)), 10.25 (0.3H, brs, CONH), 11.90 (0.7H, brs, CONH). EI-MS *m*/*z*: 232 (18), 231 ($M^{+\bullet}$, 100), 215 (56), 203 (17), 202 (19), 189 (10), 188 (20), 175 (50), 173 (10), 122 (19), 121 (16), 92 (15).

Determination of hMAO Isoform Activity. The effects of the test compounds on *h*MAO isoform enzymatic activity were evaluated by a fluorimetric method following the experimental protocol previously described elsewhere.[8] Briefly, 0.1 mL of sodium phosphate buffer (0.05 M, pH 7.4) containing various concentrations of the test drugs (new compounds or reference inhibitors) and adequate amounts of recombinant *h*MAO-A or *h*MAO-B required and adjusted to obtain in our experimental conditions the same reaction velocity, i.e., to oxidize (in the control group) 165 pmol of *p*-tyramine/min (*h*MAO-A, 1.1 μg protein; specific activity, 150 nmol of *p*-tyramine oxidized to (*p*-hydroxyphenylacetaldehyde/min)/mg protein; *h*MAO-B, 7.5 μg of protein; specific activity, 22 nmol of (*p*-tyramine transformed/min)/mg protein), was incubated for 15 min at 37 °C in a flat-black-bottom 96-well microtest plate (BD Biosciences, Franklin Lakes, NJ, U.S.) placed in a dark multimode microplate reader chamber. After this incubation period, the reaction was started by adding (final concentrations) 200 μM Amplex Red reagent, 1 U/mL horseradish peroxidase, and 1 mM *p*-tyramine. The production of H_2O_2 and consequently of resorufin was quantified at 37 °C in a multimode microplate reader (Fluostar Optima, BMG Labtech GmbH, Offenburg, Germany), based on the fluorescence generated (excitation, 545 nm, emission, 590 nm) over a 15 min period, in which the fluorescence increased linearly.

Control experiments were carried out simultaneously by replacing the test drugs (new compounds and reference inhibitors) with appropriate dilutions of the vehicles. In addition, the possible capacity of the above test drugs to modify the fluorescence generated in the reaction mixture due to nonenzymatic inhibition (e.g., for directly reacting with Amplex Red reagent) was determined by adding these drugs to solutions containing only the Amplex Red reagent in a sodium phosphate buffer.

To determine the kinetic parameters of *h*MAO-A and *h*MAO-B (K_m and V_{max}), the corresponding enzymatic activity of both isoforms was evaluated (under the experimental conditions described above) in the presence of a number (a wide range) of *p*-tyramine concentrations.

The specific fluorescence emission (used to obtain the final results) was calculated after subtraction of the background activity, which was determined from vials containing all components except the MAO isoforms, which were replaced by a sodium phosphate buffer solution.

Reversibility and Irreversibility Experiments. To evaluate whether compounds **15** and **19** are reversible or irreversible *h*MAO-B inhibitors, an effective centrifugation−ultrafiltration method (so-called repeated washing) was used.[8] Briefly, adequate amounts of the recombinant *h*MAO-B were incubated with a single concentration (see Table 2) of the compounds **15** and **19** or the reference inhibitors *R*-(−)-deprenyl and isatin in a sodium phosphate buffer (0.05 M, pH 7.4) for 15 min at 37 °C. After this incubation period, an aliquot of this incubated mixture was stored at 4 °C and used for subsequent measurement of *h*MAO-B activity under the experimental conditions indicated above (see the section on determination of MAO activity). The remaining incubated sample (300 μL) was placed in an Ultrafree-0.5 centrifugal tube (Millipore, Billerica, MA, U.S.) with a 30 kDa Biomax membrane in the middle of the tube and centrifuged (9000*g*,

20 min, 4 °C) in a centrifuge (J2-MI, Beckman Instruments, Inc., Palo Alto, CA, U.S.). The enzyme retained in the 30 kDa membrane was resuspended in sodium phosphate buffer at 4 °C and centrifuged again (under the same experimental conditions described above) two successive times. After the third centrifugation, the enzyme retained in the membrane was resuspended in sodium phosphate buffer (300 μL) and an aliquot of this suspension was used for subsequent *h*MAO-B activity determination. Similar studies were carried out on MAO-A activity in the presence of the reference inhibitor moclobemide under the experimental conditions described above.

Control experiments were performed simultaneously (to define 100% *h*MAO activity) by replacing the test drugs with appropriate dilutions of the vehicles. The corresponding values of percent *h*MAO inhibition were separately calculated for samples with and without repeated washing.

Statistical Analysis of Data. Data were expressed as the mean (±SEM) and were analyzed by ANOVA followed by Dunnett's test. Groups of test data (mean ± SD) were comparing using the Student's *t* test for paired observations. Values were considered to differ significantly at the level of $p < 0.05$.

Molecular Modeling. The most active and selective compound **19** was built by means of the Maestro[21] and energy minimized with 2000 steps of Polak−Ribiere conjugated gradient algorithm applied to OPLS-2005 force field[22] as implemented in MacroModel.[23]Solvating effects were simulated by means of the GB/SA[24] water implicit model as implemented in the same program. Docking simulations were carried out using the ligand flexible algorithm of Glide.[18]The target models of hMAO-A and hMAO-B were obtained from two Protein Data Bank high resolution crystal structures 2Z5X[19] and 2V5Z,[20] respectively. After removal of cocrystallized ligands, harmine for 2Z5X and safinamide for 2V5Z, the binding sites were defined by means of a regular box of about 1000 Å^3 centered onto the N5 FAD cofactor. Glide XP scoring function was adopted for stability evaluation of the complexes. The quality of our protocols has been evaluated by submitting the X-ray cocrystallized ligands to redocking. In both *h*MAO-A and -B cases the theoretical complexes were almost identical to the experimental ones, as reported by the root mean square deviation equal to 0.26 and 0.21 Å, respectively.

In order to take into account the solvation effects of the other compounds **3**−**10** and **15**−**22**, models of these derivatives were submitted to 1000 iterations of Monte Carlo conformational search as implemented in MacroModel[23] and energy minimized with the same protocol, force field, and implicit model of solvation considered for the most selective compound **19**.

AUTHOR INFORMATION

Corresponding Author

*For S.A.: phone, +39 09613694197; fax, +39 0961391490; e-mail, alcaro@unicz.it. For F.B.: phone, +351 220402560; fax, +351 220402659; e-mail, fborges@fc.up.pt.

ACKNOWLEDGMENT

This work was supported by the Foundation for Science and Technology (FCT), Portugal (Projects PTDC/QUI/70359/2006 and PTDC/QUI-QUI/113687/2009). A.G. (Grant SFRH/BD/43531/2008) and F.B. (Grant SFRH/BSAB/1090/2010) are thankful for the FCT grants. The authors are grateful to Dr. Alfredo Mellace (Department of Chemistry, Nassau Community College NY, USA) for proofreading the revised manuscript.

DEDICATION

†This article is dedicated to the memory of Prof. Francisco Orallo, the pharmacologist and friend who believed in us.

ABBREVIATIONS USED

CNS, central nervous system; FAD, flavin adenine dinucleotide; MAO, monoamine oxidase; MAO-A, monoamine oxidase A; MAO-B, monoamine oxidase B; *h*MAO, human MAO isoform; PDB, Protein Data Bank; SAR, structure−activity relationship

REFERENCES

(1) (a) Reyes-Parada, M.; Fierro, A.; Iturriaga-Vásquez, A. P.; Cassels, B. K. Monoamine oxidase inhibition in the light of new structural data. *Curr. Enzyme Inhib.* **2005**, *1*, 85–95. (b) Pacher, P.; Kecskeméti, V. Trends in the development of new antidepressants. Is there a light at the end of the tunnel? *Curr Med. Chem.* **2004**, *11*, 925–943. (c) Edmondson, D. E.; Mattevi, A.; Binda, C.; Li, M.; Hubalek, F. Structure and mechanism of monoamine oxidase. *Curr. Med. Chem.* **2004**, *11*, 1983–1993. (d) Riederer, P.; Lachenmayer, L.; Laux, G. Clinical applications of MAO-inhibitors. *Curr. Med. Chem.* **2004**, *11*, 2033–2043.

(2) Rigby, S. E.; Basran, J.; Combe, J. P.; Mohsen, A. W.; Toogood, H.; van Thiel, A.; Sutcliffe, M. J.; Leys, D.; Munro, A. W.; Scrutton, N. S. Flavoenzyme catalysed oxidation of amines: roles for flavin and protein-based radicals. *Biochem. Soc. Trans.* **2005**, *33*, 754–757.

(3) Bertoni, J.; Elmer, L. The Role of MAO-B Inhibitors in the Treatment of Parkinson's Disease. In *Parkinson's Disease*; Ebadi, M., Pfeiffer, R. F., Eds.; CRC Press: Boca Raton, FL, 2005; pp 691−704.

(4) Lang, A. E.; Lees, A. MAO-B inhibitors for the treatment of Parkinson's disease. *Mov. Disord.* **2002**, *17*, S38–S44.

(5) (a) Husain, M.; Shukla, R.; Dikshit, M.; Maheshwari, P. K.; Nag, D.; Srimal, R. C.; Seth, P. K.; Khanna, V. K. Altered platelet monoamine oxidase-B activity in idiopathic Parkinson's disease. *Neurochem. Res.* **2009**, *34*, 1427–1432. (b) Chen, J. J.; Swope, D. M.; Dashtipour, K. Comprehensive review of rasagiline, a second generation monoamine oxidase inhibitor, for the treatment of Parkinson's disease. *Clin. Ther.* **2007**, *29*, 1825–1846.

(6) (a) Deeb, O.; Alfalah, S.; Clare, B. W. QSAR of aromatic substances: MAO inhibitory activity of xanthone derivatives. *J. Enzyme Inhib. Med. Chem.* **2007**, *22*, 277–286. (b) Thull, U.; Kneubühler, S.; Testa, B.; Borges, M. F.; Pinto, M. M. Substituted xanthones as selective and reversible monoamine oxidase A (MAO-A) inhibitors. *Pharm. Res.* **1993**, *10*, 1187–1190.

(7) (a) Santana, L.; González-Díaz, H.; Quezada, E; Uriarte, E.; Yáñez, M.; Viña, D.; Orallo, F. Quantitative structure−activity relationship and complex network approach to monoamine oxidase A and B inhibitors. *J. Med. Chem.* **2008**, *51*, 6740–6751. (b) Binda, C.; Wang, J.; Pisani, L.; Caccia, C.; Carotti, A.; Salvati, P.; Edmondson, D. E.; Mattevi, A. Structures of human monoamine oxidase B complexes with selective noncovalent inhibitors: safinamide and coumarin analogs. *J. Med. Chem.* **2007**, *50*, 5848–5852. (c) Catto, M.; Nicolotti, O.; Leonetti, F.; Carotti, A.; Favia, A. D.; Soto-Otero, R.; Mendez-Alvarez, E.; Carotti, A. Structural insights into monoamine oxidase inhibitory potency and selectivity of 7-substituted coumarins from ligand- and target-based approaches. *J. Med. Chem.* **2006**, *49*, 4912–4925. (d) Borges, F.; Roleira, F.; Milhazes, N.; Santana, L.; Uriarte, E. Simple coumarins and analogues in medicinal chemistry: occurrence, synthesis and biological activity. *Curr. Med. Chem.* **2005**, *12*, 887–916.

(8) (a) Chimenti, F.; Secci, D.; Bolasco, A.; Chimenti, P.; Bizzarri, B.; Granese, A.; Carradori, S.; Yáñez, M.; Orallo, F.; Ortuso, F.; Alcaro, S. Synthesis, molecular modeling, and selective inhibitory activity against human monoamine oxidases of 3-carboxamido-7-substituted coumarins. *J. Med. Chem.* **2009**, *52*, 1935–1942. (b) Chimenti, F.; Fioravanti, R.; Bolasco, A.; Chimenti, P.; Secci, D.; Rossi, F.; Yáñez, M.; Orallo, F.; Ortuso, F.; Alcaro, S. Chalcones: a valid scaffold for monoamine oxidases inhibitors. *J. Med. Chem.* **2009**, *52*, 2818–2824. (c) Chimenti, F.; Fioravanti, R.; Bolasco, A.; Chimenti, P.; Secci, D.; Rossi, F.; Yáñez, M.; Orallo, F.; Ortuso, F.; Alcaro, S.; Cirilli, R.; Ferretti, R.; Sanna, M. L. A new series of flavones, thioflavones, and flavanones as selective monoamine oxidase-B inhibitors. *Bioorg. Med. Chem.* **2010**, *18*, 1273–1279.

(9) Ellis, G. P., Ed. *The Chemistry of Heterocyclic Compounds, Chromenes, Chromanones and Chromones*; J. Wiley & Sons: New York, 2007; Vol. 31.

(10) (a) Ishar, M. P. S.; Singh, G.; Singh, S.; Sreenivasan, K. K.; Singh, G. Design, synthesis, and evaluation of novel 6-chloro-fluorochromone derivatives as potential topoisomerase inhibitor anticancer agents. *Bioorg. Med. Chem. Lett.* **2006**, *16*, 1366–1370. (b) Peixoto, F.; Barros, A. I. R. N. A.; Silva, A. M. S. Interactions of a new 2-styrylchromone with mitochondrial oxidative phosphorylation. *J. Biochem. Mol. Toxicol.* **2002**, *16*, 220–226. (c) Ellis, G. P.; Barker, G. 2. Chromones-2- and -3-carboxylic acids and their derivatives. *Prog. Med. Chem.* **1972**, *9*, 65–116. (d) Alcaro, S.; Gaspar, A.; Ortuso, F.; Milhazes, N.; Orallo, F.; Uriarte, E.; Yáñez, M.; Borges, F. Chromone-2- and -3-carboxylic acids inhibit differently monoamine oxidases A and B. *Bioorg. Med. Chem. Lett.* **2010**, *20*, 2709–2712. (e) Desideri, N.; Bolasco, A.; Fioravanti, R.; Proietti Monaco, L.; Orallo, F.; Yáñez, M.; Ortuso, F.; Alcaro, S. Homoisoflavonoids: natural scaffolds with potent and selective monoamine oxidase-B inhibition properties. *J. Med. Chem.* **2011**, *54*, 2155–2164.

(11) (a) Borges, M. F. M.; Gaspar, A. M. N.; Garrido, J. M. P. J.; Milhazes, N. J. S. P.; Batoreu, M. C. C. Chromone Derivatives for Use as Antioxidants/Preservatives. WO 2008/104925 A1, 2008; Universidade do Porto, Port, Portugal (*Chem. Abstr.* **2008**, *149*, 332206). (b) Borges, M. F.; Gaspar, A. M. N.; Garrido, J. M. P. J.; Milhazes, N.J.S.P; Uriarte, E.; Yáñez, M.; Orallo, F. Utilização de Cromonas, Seus Derivados, Seus Sais Farmaceuticamente Aceitáveis e Seus Pró-Fármacos com Actividade Inibidora da Monoamina Oxidase e Aplicações Terapêuticas Relacionadas. Priority Data PT 104487, 2009; Universidade do Porto, Port, Portugal. (c) Gaspar, A.; Reis, J.; Fonseca, A.; Milhazes, N.; Viña, D.; Uriarte, E.; Borges, M. F. Chromone 3-phenylcarboxamides as potent and selective MAO-B inhibitors. *Bioorg. Med. Chem. Lett.* **2011**, *21*, 707–709.

(12) Berman, H. M.; Westbrook, J.; Feng, Z.; Gilliland, G.; Bhat, T. N.; Weissig, H.; Shindyalov, I. N.; Bourne, P. E. The Protein Data Bank. *Nucleic Acids Res.* **2000**, *28*, 235–242.

(13) Dormoy, J. R.; Castro, B. The reaction of hexamethyl phosphoric triamide (HMPT) with phosphoryl chloride: a reexamination. Application to a novel preparation of BOP reagent for peptide coupling. *Tetrahedron Lett.* **1979**, *20*, 3321–3322.

(14) *Comprehensive Organic Synthesis: Selectivity, Strategy and Efficiency in Modern Organic Chemistry*; Trost, B. M., Fleming, I., Winterfeldt, E., Eds.; Pergamon Press: Oxford, U.K., 1991; Vol. 6.

(15) Matos, M. J.; Viña, D.; Quezada, E.; Picciau, C.; Delogu, G.; Orallo, F.; Santana, L.; Uriarte, E. A new series of 3-phenylcoumarins as potent and selective MAO-B inhibitors. *Bioorg. Med. Chem. Lett.* **2009**, *19*, 3268–3270.

(16) Gerlach, M.; Riederer, P.; Youdim, M. B. The molecular pharmacology of L-deprenyl. *Eur. J. Pharmacol.* **1992**, *226*, 97–108.

(17) Gaspar, A.; Teixeira, F.; Uriarte, E.; Milhazes, N.; Melo, A.; Cordeiro, M. N.; Ortuso, F.; Alcaro, S.; Borges, F. Towards the discovery of a novel class of monoamine oxidase inhibitors: structure—property—activity and docking studies on chromone amides. *ChemMedChem* **2011**, *6*, 628–32.

(18) (a) *Glide*, version 5.6; Schrodinger, LLC: New York, NY, 2010. (b) Friesner, R. A.; Banks, J. L.; Murphy, R. B.; Halgren, T. A.; Klicic, J. J.; Mainz, D. T.; Repasky, M. P.; Knoll, E. H.; Shaw, D. E.; Shelley, M.; Perry, J. K.; Francis, P.; Shenkin, P. S. Glide: a new approach for rapid, accurate docking and scoring. 1. Method and assessment of docking accuracy. *J. Med. Chem.* **2004**, *47*, 1739–1749. (c) Halgren, T. A.; Murphy, R. B.; Friesner, R. A.; Beard, H. S.; Frye, L. L.; Pollard, W. T.; Banks, J. L. Glide: a new approach for rapid, accurate docking and scoring. 2. Enrichment factors in database screening. *J. Med. Chem.* **2004**, *47*, 1750–1759. (d) Friesner, R. A.; Murphy, R. B.; Repasky, M. P.; Frye, L. L.; Greenwood, J. R.; Halgren, T. A.; Sanschagrin, P. C.; Mainz, D. T. Extra precision glide: docking and scoring incorporating a model of hydrophobic enclosure for protein—ligand complexes. *J. Med. Chem.* **2006**, *49*, 6177–6196. (e) Park, M.; Gao, C.; Stern, H. A. Estimating binding affinities by docking/scoring methods using variable protonation states. *Proteins* **2010**, *79*, 304–314.

(19) Son, S. Y.; Ma, J.; Kondou, Y.; Yoshimura, M.; Yamashita, E.; Tsukihara, T. Structure of human monoamine oxidase A at 2.2 Å resolution: the control of opening the entry for substrates/inhibitors. *Proc. Natl. Acad. Sci. U.S.A.* **2008**, *105*, 5739–5744; data deposition at www.pdb.org (PDB code 2Z5X).

(20) Binda, C.; Wang, J.; Pisani, L.; Caccia, C.; Carotti, A.; Salvati, P.; Edmondson, D. E.; Mattevi, A. Structures of human monoamine oxidase B complexes with selective noncovalent inhibitors: safinamide and coumarin analogs. *J. Med. Chem.* **2007**, *50*, 5848–5852; data deposition at www.pdb.org (PDB code 2V5Z).

(21) *Maestro*, version 9.1; Schrodinger, LLC: New York, NY, 2010.

(22) Kaminski, G.; Friesner, R. A.; Tirado-Rives, J.; Jorgensen, W. L. Evaluation and reparametrization of the OPLS-AA force field for proteins via comparison with accurate quantum chemical calculations on peptides. *J. Phys. Chem. B* **2001**, *105*, 6474–6487.

(23) (a) *MacroModel*, version 9.8; Schrodinger, LLC, New York, NY, 2010. (b) Mohamadi, F.; Richards, N. G. J.; Guida, W. C.; Liskamp, R.; Lipton, M.; Caufield, C.; Chang, G.; Hendrickson, T.; Still, W. C. MacroModel—an integrated software system for modeling organic and bioorganic molecules using molecular mechanics. *J. Comput. Chem.* **1990**, *11*, 440–467.

(24) Hasel, W.; Hendrickson, T. F.; Still, W. C. A rapid approximation to the solvent accessible surface areas of atoms. *Tetrahedron Comput. Methodol.* **1988**, *1*, 103–116.